Bidirectional Electron Transfer in Photosystem I: Accumulation of A_0^- in A-Side or B-Side Mutants of the Axial Ligand to Chlorophyll A_0†

V. M. Ramesh,[‡,§] Krzysztof Gibasiewicz,[‡,§,||] Su Lin,[§,⊥] Scott E. Bingham,[‡,§] and Andrew N. Webber*[,‡,§]

School of Life Sciences, Department of Chemistry and Biochemistry, and Center for the Study of Early Events in Photosynthesis, Arizona State University, Tempe, Arizona 85287, and Institute of Physics, A. Mickiewicz University, ul. Umultowska 85, 61-614 Poznan, Poland

Received August 7, 2003; Revised Manuscript Received November 6, 2003

ABSTRACT: Photosystem I contains two potential electron transfer pathways between P_{700} and F_X. These branches are made up of the electron transfer chain components A, A_0, and A_1. The primary electron acceptor A_0 is a chlorophyll *a* monomer that could be one or both of the two chlorophyll molecules, eC-A_3/eC-B_3, identified in the 2.5 Å resolution structure. The eC-A_3/eC-B_3 chlorophylls are both coordinated by the sulfur atom of a methionine. This coordination is highly unusual, as interactions between the acid Mg^{2+} and the soft base sulfur are weak. The eC-A_3/eC-B_3 chlorophylls also are located close to one of the connecting chlorophylls that may link the antenna and the electron transfer chain chlorophylls. Due to their location in the structure, the eC-A_3/eC-B_3 chlorophylls may play a role in both excitation energy transfer and electron transfer. To test the role of the eC-A_3/eC-B_3 chlorophylls in electron transfer, Met-684 of PsaA and Met-664 of PsaB have been changed to His, Ser, and Leu. Replacement of either M(A684) or M(B664) results in a significant alteration in growth phenotype. The His and Leu mutants are very light sensitive in the presence of oxygen. Growth is impaired to a greater extent in the B-side mutants. However, all of the mutants are able to grow anaerobically at comparable rates. The His and Ser mutants all accumulate PSI at a level similar to that of wild type, whereas the Leu mutants have reduced amounts of PSI. Ultrafast transient absorbance measurements show that the ($A_0^- - A_0$) difference signal accumulates in the MH(A684) and MH(B664) mutants under neutral conditions, demonstrating that electron transfer between A_0^- and A_1 is blocked or significantly slowed. The results show that both the A-branch and the B-branch of the ETC are active in PSI from *Chlamydomonas reinhardtii*.

Photosystem I (PSI)[1] is a multisubunit pigment−protein complex that catalyzes the light-induced electron transfer from plastocyanin/cytochrome c_6 on the lumenal side of the membrane to ferredoxin or flavodoxin on the stromal side of the membrane (*1*, *2*). The X-ray structure of PSI from *Synechococcus elongates* at 2.5 Å resolution (*3*) reveals 12 protein subunits, 96 chlorophylls (Chls), 22 carotenoids (Cars), 2 phylloquinones, 3 iron−sulfur clusters, 4 lipids, ∼200 water molecules, and 1 metal ion (presumably Ca^{2+}). The reaction center core is formed by two homologous proteins, PsaA and PsaB, each having 11 transmembrane helices (A/B-a to A/B-k). The six N-terminal transmembrane α-helices, A/B-a to A/B-f, of these subunits bind the antenna Chls, whereas the remaining five C-terminal transmembrane α-helices, A/B-g to A/B-k, surround the electron transport chain (ETC) and provide ligands for its components: the primary donor P_{700}, a Chl *a*/Chl *a*′ dimer; two accessory Chls, A; two Chl *a* monomers, A_0; two phylloquinones, A_1; and the iron−sulfur cluster F_X. The terminal electron acceptors F_A and F_B are bound to the PsaC subunit on the lumenal side of the thylakoid membrane.

The ETC is arranged in two quasi-symmetrical branches and consists of six Chls, two phylloquinones (A_1), and three Fe_4S_4 clusters (F_X, F_A, and F_B) (*3*). The first pair of Chls is P_{700} (eC-A1/eC-B1) and the second pair auxiliary Chls (eC-B2/eC-A2). One or both of the Chl *a* molecules of the third pair of Chls (eC-A3/eC-B3) represents the first spectroscopically resolved electron acceptor A_0. Although the electron transfer components of the PSI reaction center are well characterized, it has been difficult to unequivocally define the route of electron transfer. Analogy of the structure of PSI to that of the purple bacteria reaction center has led to suggestions that electron transfer would occur preferentially along one branch. Alternatively, the fact that PSI is related to bacterial type I reaction centers, which are homodimers, and the nearly perfect symmetry of the PSI ETC suggest that electron transfer should occur along either branch. However, ENDOR studies of mutants of the residues binding P_{700} have shown that the Chl on the PsaB side carries

† This work was supported by the National Research Initiatives Competitive Grants Program of the USDA (2001-35318-11137).

* Address correspondence to this author at the School of Life Sciences, P.O. Box 874501, Arizona State University. Phone: (480) 965-8725. Fax: (480) 965-6899. E-mail: andrew.webber@asu.edu.

‡ School of Life Sciences, Arizona State University.

§ Center for the Study of Early Events in Photosynthesis, Arizona State University.

|| Institute of Physics, A. Mickiewicz University.

⊥ Department of Chemistry and Biochemistry, Arizona State University.

[1] Abbreviations: A_0, primary electron acceptor in photosystem I (chlorophyll *a* monomer); A_1, phylloquinone secondary electron acceptor in photosystem I; ENDOR, electron nuclear double resonance; EPR, electron paramagnetic resonance; ETC, electron transport chain; F_A, F_B, and F_X, iron−sulfur centers of photosystem I; PMS, phenazine methosulfate; PSI, photosystem I; P700, primary electron donor of photosystem I.

10.1021/bi0354177 CCC: $27.50
Published on Web 01/13/2004

most of the electron spin density in the cation P_{700}^+ (*4*, *5*). This indicates that, despite the nearly perfect symmetry of the two branches in the structure, there can still be quite dramatic differences in the electronic characteristics of the two branches.

Most of the evidence for one or two active branches has come from studying the accumulation or reoxidation of the quinone acceptor A_1. EPR experiments at low temperature and reducing conditions detect only a single quinone (*6*, *7*), and a mutant of *Synechococcus* sp. PCC 7002 lacking the PsaE and PsaF subunits normally associated with PsaA only accumulates A_0^- and not A_1^-, suggesting the active quinone is on the A-side (*8*). Using spin-polarized EPR on single crystals of PSI, the distance between this reduced quinone and P_{700}^+ has been precisely measured and shows that the A_1^- must be located on the opposite side to the Chl cation of P_{700}^+ (*6*, *7*). This means that the PsaA branch contains the active quinone. These results have been challenged by observations of the biphasic nature of quinone reoxidation (*1*) and reports that two quinones can be detected under reducing conditions (*9*, *10*). Joliot and Joliot (*11*) measured the rate of phylloquinone oxidation in whole cells of the green alga *Chlorella pyrenoidosa* and found two rates of oxidation, $t_{1/e} = 13$ and 140 ns at room temperature. They suggested that electron transfer is in fact bidirectional, and initial electron transfer is randomly directed to either side of the reaction center, with the overall rate limited on each side by the A_1 to F_X rate. This suggestion is supported by analysis of the site-directed mutants PsaA W693F and PsaB W673F in *Chlamydomonas reinhardtii* (*12*) that alter the A_1 binding pocket on the PsaA and PsaB side, respectively. The fast phase of 13 ns was slowed by the PsaB side mutation to 70 ns, and the 140 ns rate was slowed to 490 ns by the PsaA mutation (*12*), supporting their contention that both phylloquinones are active. However, reduction of Qk-B by alternative electron transfer pathways, perhaps by electrons from Qk-A via F_X, cannot be completely ruled out (*1*).

In the present investigation we have addressed whether electron transfer proceeds along the A- and/or B-branch by changing the methionine residue that provides a ligand to the central magnesium of eCA-3 or eCB-3, respectively, in *C. reinhardtii*. Using fast optical spectroscopy we show that the mutation of either Met blocks or significantly slows electron transfer along the respective branch, causing accumulation of A_0^-, supporting the view of bidirectional electron transfer in *Chlamydomonas* PSI.

MATERIALS AND METHODS

Site-Directed Mutagenesis and Transformation of Chloroplasts. Oligonucleotide-mediated site-directed mutagenesis was used to introduce mutations into the *psaA* or *psaB* gene. The Met A684 and Met B664 axial ligands to primary electron acceptor A_0 were replaced with histidine, leucine, and serine using protocols essentially as described previously (*4*, *13*). The *C. reinhardtii* recipient strains for transformation were CC125 (wild-type mt^+) obtained from the *Chlamydomonas* Culture Collection at Duke University. Chloroplast transformation was performed by the bioballistics technique as previously described (*14*, *15*). Bombarded cells were transferred to plates containing CC media (*13*) supplemented with 100 μg mL^{-1} spectinomycin and 1.2% agar and placed under dim light for 7−10 days until colonies appeared. Single transformant colonies were restreaked onto solid medium. Total DNA was isolated from cells taken from confluent regions of the plates as previously described (*15*) and resuspended at a final volume of 100 μL. One microliter of this DNA isolation was then used as a template for PCR to confirm the introduction or loss of a specific restriction enzyme site. To confirm the presence of the desired mutation, the amplified DNA from the homoplasmic strains was sequenced.

Strains and Media. CC125 and CC2696 strains and their transformants were maintained on agar plates containing CC medium (*13*). For thylakoid membrane preparation, cells were grown in CC liquid medium to (1−1.5) × 10^{-6} cells mL^{-1} at a light intensity of 50 μmol m^{-2} s^{-1}. Growth tests were initiated by spotting 15 μL of log-phase cultures onto agar plates. Anaerobiosis was established using the BioMerieux (Marcy l'Etiole, France) Generbag Anaer system according to the manufacturer's instructions using a gas supply of 90% N_2, 5% CO_2, and 5% H_2.

Isolation of Thylakoid Membranes and Protein Analysis. Thylakoid membranes were isolated from wild-type and mutant cells according to the method described in ref *16*. To determine the steady-state level of PSI in *Chlamydomonas* cells, thylakoid membranes corresponding to 30 μg of Chl were solubilized in gel-loading buffer (5% lithium dodecyl sulfate, 100 mM dithiothreitol, 10% glycerol, and 50 mM Tris, pH 8.8) and the Chl−protein complexes separated by LDS−PAGE at 4 °C. Following electrophoresis, the PSI complexes were either visualized as a green band at the top of the gel or stained with Coomassie blue (*17*).

Isolation of the PSI Complex. The PSI complex was isolated by single-step column chromatography using a weak anion exchanger as described (*5*, *18*) with slight modifications. Cells from 6 L of medium were harvested during exponential growth at a density of 2 × 10^6 cells/mL by centrifugation at 4 °C for 10 min at 6000*g* in a Sorvall GS-3 rotor. The pellets were suspended in 350 mL of buffer A [50 mm HEPES, pH 7.2, 5 mM $MgCl_2$, 5 mM $CaCl_2$, 20% glycerol (v/v)] and centrifuged for 15 min at 9000*g* in a Sorvall GS-3 rotor. The resulting pellets were resuspended in 125 mL of the same buffer (A) containing 1 mM benzamidine, 1 mM phenylmethanesulfonyl fluoride (PMSF), and 1 mM EDTA at 2 × 10^8 cells/mL. Cells were broken in a chilled French press at 660 kg/cm^2 pressure. Unbroken cells and starch granules were removed from the membrane suspension by centrifugation for 5 min at 2000*g* in a Sorvall SS-34 rotor. Crude thylakoid membranes in the supernatant were pelleted by centrifugation at 100000*g* for 20 min in a Beckman 50.2 Ti rotor at 4 °C.

The membrane pellets were washed once with buffer A containing 1 mM benzamidine, 1 mM PMSF, and 1 mM EDTA and resuspended in the same buffer (A) at a Chl concentration of 0.6−1 mg mL^{-1}. A 10% stock solution of dodecyl maltoside (Sigma) was added dropwise to this suspension of thylakoid membranes to give a final concentration of 0.6% detergent. Extraction proceeded in the dark for 15 min on ice with gentle stirring. The suspension was then centrifuged at 125000*g* in a Beckman 50.2 Ti rotor for 20 min at 4 °C. The supernatant was loaded onto a DEAE Toyopearl 650 S column (2.7 × 26 cm, a weak anion exchanger; Toso Haas) previously equilibrated with 500 mL of buffer A containing 1 mM benzamidine, 1 mM PMSF,

and 1 mM EDTA plus 0.03% dodecyl maltoside. The column was washed successively with 600 mL of buffer A and with 500−600 mL of buffer B [50 mM HEPES, pH 7.2, 5 mM $MgCl_2$, 12 mM $CaCl_2$, 20% glycerol (v/v)] containing 1 mM benzamidine, 1 mM PMSF, and 1 mM EDTA plus 0.03% dodecyl maltoside and then with 150 mL of 5 mM $MgSO_4$ in buffer B at a flow rate of 6−7 mL/min using a peristaltic pump (Model P- 3, Pharmacia). The wash with buffer A, buffer B, and 5 mM $MgSO_4$ in buffer B elutes successively the free pigments, mainly the carotenoids. Then a 500 mL linear gradient from 5 to 25 mM $MgSO_4$ in buffer B was applied to the column. Fractions were collected in 3−5 mL each using a fraction collector (RediFrac, Pharmacia). The eluted fractions were scanned between 400 and 800 nm in a Shimadzu UV 160 spectrophotometer. Fractions with Chl absorbance maxima between 675 and 677 nm were pooled and concentrated to the desired concentration using a Centricon 100 (Amicon) at 3000*g* in a Sorvall SS-34 rotor at 4 °C.

Femtosecond Transient Absorption Measurements. Femtosecond transient absorption measurements were performed as described earlier (*18*−*20*). For experiments at room temperature, the primary donor was kept neutral during repetitive excitation by addition of 20 mM sodium ascorbate and 10 μM phenazine methosulfate. At 20 K, the concentrations of reducing chemicals were doubled. Reducing conditions, aiming at reduction of phylloquinones, were obtained by suspending the sample in 200 mM glycine buffer, pH = 11, containing 20 mM sodium ascorbate, 10 μM phenazine methosulfate, and 30 mM sodium dithionite added to the sample after degassing (*21*). The ΔA spectra of charge-separated states were collected 200 and 300 ps after excitation and averaged together (no temporal evolution of the spectra was detected between 200 and 300 ps).

RESULTS

Growth Characteristics. To determine how the mutations alter the growth characteristics of different transformants, spot tests were performed under phototrophic and heterotrophic conditions (Figure 1). All of the mutants derived from CC125 were capable of heterotrophic growth at low light (25−40 μmol of photons m^{-2} s^{-1}) when acetate was supplied. However, the MH(B664) and ML(B664) mutants could not grow heterotrophically under high light (200−250 μmol of photons m^{-2} s^{-1}), and the corresponding A-side mutants could grow only very slowly. Autotrophic growth was severely impaired in all of the mutants in the presence of oxygen. The histidine [MH(B664)] and leucine [ML(B664)] mutants failed to grow under high light and grew poorly under low light, whereas the MS(B664) could grow slowly under high light. Again, the A-side mutants were less light sensitive but still grew slower than the wild type. Removal of oxygen allowed autotrophic growth of all the mutants (Figure 1). This suggests that a functional PSI complex is present in each mutant and that the site-directed changes introduced into the PSI core result in increased photooxidative damage.

PSI Accumulation and Activity. The steady-state level of PSI in WT and transformants of *Chlamydomonas* was determined by nondenaturing LDS−PAGE. Thylakoid membranes were isolated from the wild-type and transformant cells and the Chl−protein complexes separated by LDS−PAGE at 4 °C. The PSI complex can be clearly visualized as a green band near the top of the gel, which can also be stained with Coomassie blue. As shown in Figure 2, the MH(A684), MS(A684), MH(B664) and MS(B664) mutants accumulated similar levels of PSI as the wild-type cells, whereas replacement of Met by the structurally similar Leu resulted in a decreased PSI level.

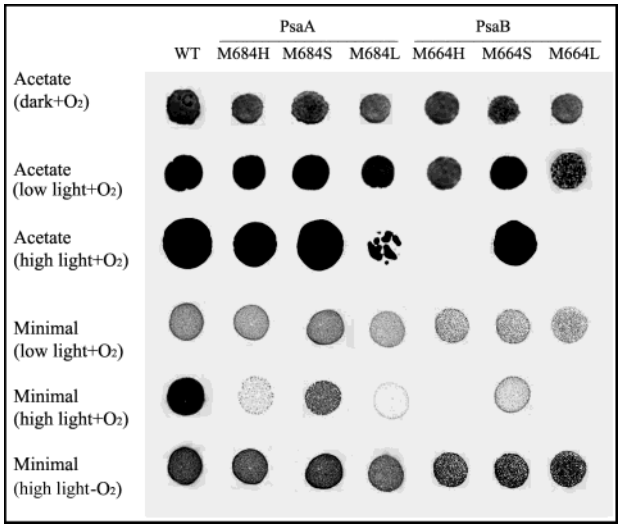

FIGURE 1: Spot tests of mutants of *C. reinhardtii* growing on acetate and minimal medium. Acetate indicates TAP medium and supports heterotrophic growth, whereas minimal medium will only support phototrophic growth. Colonies were allowed to develop in darkness and in 25−40 (low) or 250 (high) μmol of photons m^{-2} s^{-1} light and in the presence or absence of oxygen as indicated.

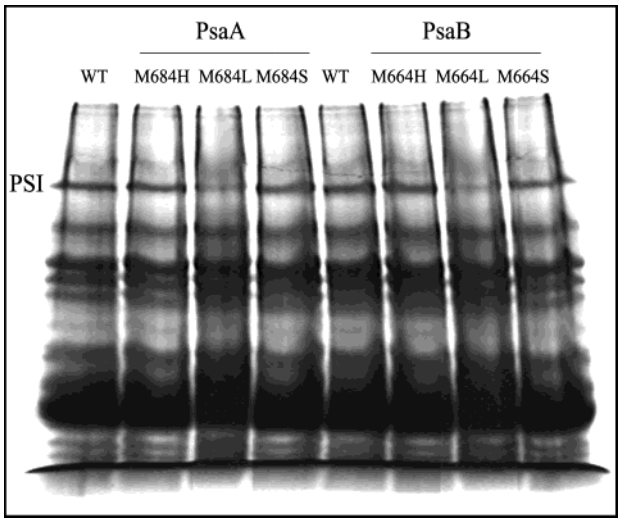

FIGURE 2: Accumulation of PSI in thylakoid membranes determined by LDS nondenaturing PAGE. Each lane was loaded with 30 μg of Chl.

Mutations Cause Accumulation of A_0^- under Nonreducing Conditions. Normally the steady-state level of A_0^- is too low to be detected. However, under reducing conditions that cause accumulation of A_1^- it is possible to also accumulate A_0^-. Figure 3 shows difference spectra recorded at 200−300 ps after excitation at 695 nm for PSI preparations from the wild type and the MH(A684) and MH(B664) mutants under neutral conditions (i.e., with P_{700} neutral before each excitation). Interestingly, the shapes of the two spectra for mutants are different from the wild type in the ~682 nm

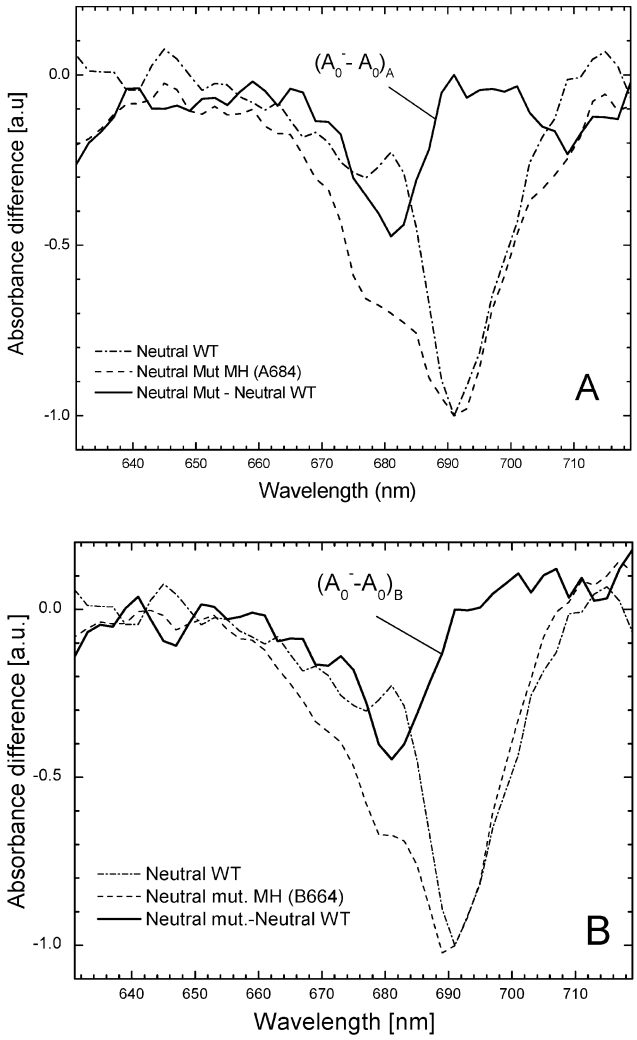

FIGURE 3: Extraction of $(A_0^- - A_0)$ absorbance difference spectra in the MH(A684) (A) and MH(B664) (B) mutant PSI from *C. reinhardtii* measured at room temperature under neutral conditions. The spectra presented were recorded 200−300 ps after ∼150 fs excitation at 695 nm. (Laser pulse frequency is 1 kHz. At room temperature, a wheel rotating with a rotation frequency of ∼2 Hz ensures that each laser flash excites a fresh/relaxed sample.) See text for further details.

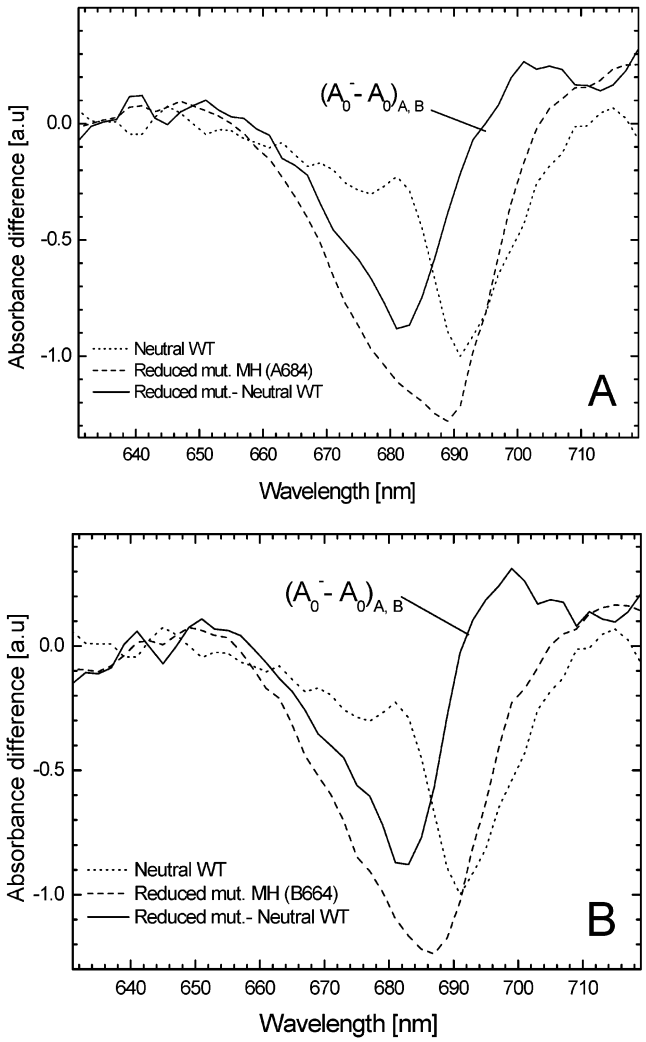

FIGURE 4: Absorption difference spectrum of MH(A684) (A) and MH(B664) (B) under reducing conditions, recorded 200−300 ps after ∼150 fs excitation at 695 nm at room temperature. The difference spectrum marked $(A_0^- - A_0)_{A,B}$ was obtained by subtraction of the spectrum measured in WT under neutral conditions [assigned to the $(P^+ - P)$ spectrum] from the spectrum measured in the mutant under reducing conditions [assigned to the $(P^+A_0^- - PA_0)$ spectrum]. (Laser pulse frequency is 1 kHz. At room temperature, a wheel rotating with a rotation frequency of ∼2 Hz ensures that each laser flash excites a fresh/relaxed sample.) See text for further details.

region (Figure 3). The $\Delta\Delta A$ signals resulting from subtraction of the wild-type trace from the mutant trace are shown as solid lines and represent the differences in the charge-separated states detected in both samples and are attributed to accumulation of A_0^-; i.e., it should be the A_0^- accumulating in the mutant.

To confirm this assignment, the MH(A684) and MH(B664) mutants were treated with sodium dithionite under anaerobic conditions at pH = 11 to completely reduce A_1 and block electron transfer from A_0^- to A_1 (*21*). Figure 4 shows the ΔA signals recorded under these reducing conditions 200−300 ps after excitation (dashed lines). In the same panel the ΔA spectrum for the wild type under neutral conditions is replotted from Figure 3 (dotted lines). Under neutral conditions the wild-type spectrum contains contributions exclusively from the $(P700^+ - P700)$ signal, whereas the spectra from the MH(A684) and the MH(B664) mutants under reducing conditions contain an additional contribution from the $(A_0^- - A_0)$ signal. Thus, the difference between these two traces is ascribed to the $(A_0^- - A_0)$ difference spectrum (Figure 4, dashed lines). The similarity in the shape of the $\Delta\Delta A$ signal obtained from the MH(A684) and the MH(B664) mutants under both neutral and reducing conditions confirms that under neutral conditions A_0^- is accumulated in the mutant.

Figure 5 shows a comparison of the $(A_0^- - A_0)$ spectra extracted from the experiments with PSI mutants under reducing conditions (dotted lines) and under neutral conditions (solid traces), the latter being attributed to the A-side and the B-side A_0 Chls, respectively. In addition, there are shown for both mutants the spectra of $(A_0^- - A_0)$ attributed to the opposite A_0, not affected by the mutation. These spectra were simply calculated as differences between the $(A_0^- - A_0)$ spectra recorded under reducing and under neutral conditions. Within experimental error, the shapes of all of these traces are the same. It should be noted that exact shapes and amplitudes of the two $\Delta\Delta A$ traces will depend on the normalization of the wild-type ΔA spectra relative to

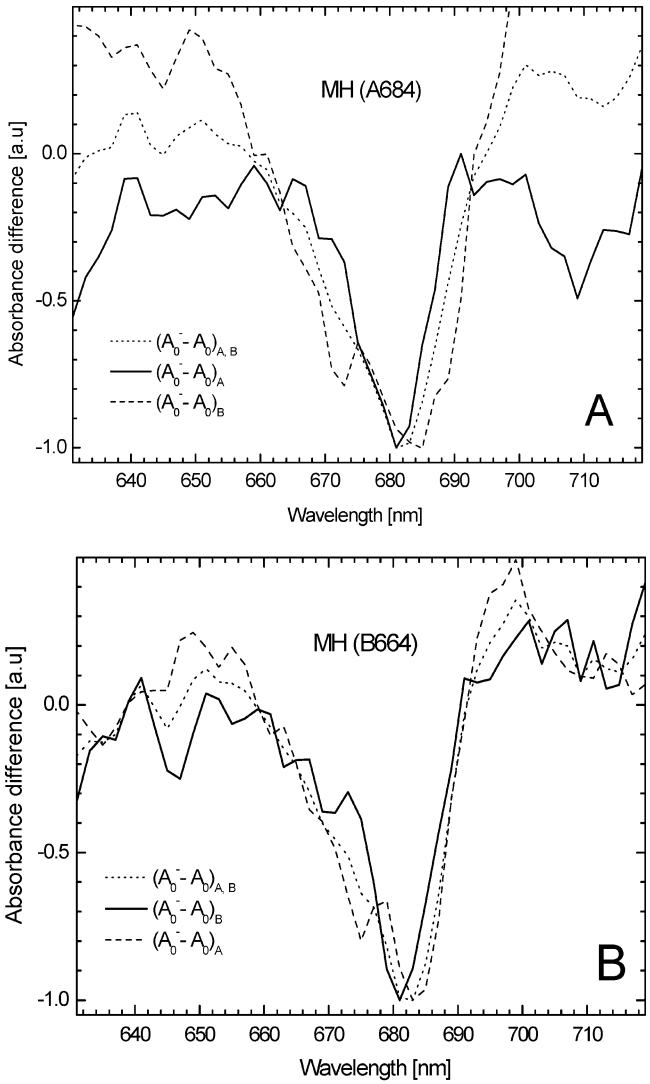

FIGURE 5: Comparison of normalized $(A_0^- - A_0)$ spectra from Figures 3 and 4 and the spectrum $(A_0^- - A_0)_B$ (panel A) or $(A_0^- - A_0)_A$ (panel B) obtained as a difference between $(A_0^- - A_0)_{A,B}$ and $(A_0^- - A_0)_A$ or a difference between $(A_0^- - A_0)_{A,B}$ and $(A_0^- - A_0)_B$. See text for further details.

the MH(A684) and the MH(B664) ΔA spectra (Figure 3). In Figure 3 it was assumed that at 691 nm the ΔA signal for the wild type is the same as for the mutant. In other words, at 691 nm only ($P700^+ - P700$) contributes to the ΔA signal. This assumption is reasonable in view of the previously published spectra of $(A_0^- - A_0)$ in PSI from *C. reinhardtii*, in which $\Delta A_{691nm} \cong 0$ (*22*). On the other hand, Melkozernov et al. (*21*), using a different normalization approach, showed some nonzero ΔA signal of $(A_0^- - A_0)$ at 691 nm. Therefore, we also constructed $\Delta\Delta A$ and $\Delta\Delta\Delta A$ spectra for different normalization factors between WT and MH(B664), decreasing the ΔA signal for WT down to 60%. However, we found that using these different normalization factors did not change significantly the shapes or maximum positions of the traces shown in Figure 5 [compare to the application of different normalization factors in Hastings et al. (*22*) and Melkozernov et al. (*21*)].

Excitonic Coupling. Following excitation at 700 nm at 20 K, wide and structured absorption difference spectra decaying on the subpicosecond time scale were observed for PSI from *Chlamydomonas* (*19*). Absorbance changes recorded 0.27−0.32 ps after excitation of WT PSI and the MH(A684) and MH(B664) mutants at 700 nm and at 20 K are shown in Figure 6. For the WT PSI, results from two different preparations are shown to illustrate reproducibility. The WT PSI spectrum has four negative bands (peaking at 667, 675, 683−685, and 695 nm) and four positive bands (peaking at 635, 645, 653, and 661 nm). These bands have been attributed to arise from excitonic interaction between eight Chls: the six ETC Chls and two connecting chlorophylls (*19*). Absorbance changes for the eC-A3 and eC-B3 mutants [MH(A684) and MH(B664)] are similar to each other but significantly different from the WT (Figure 6). The amplitude of the 683 nm band drops about twice relative to the band at 695 (697) nm and when compared to the WT. Also, the amplitudes of the 667 and 675 nm bands are smaller than those in WT. The majority of the band peaking at 695 nm (Figure 6) comes from molecules that are not coupled to the group of molecules responsible for the remaining part of spectral features between 630 and 700 nm.

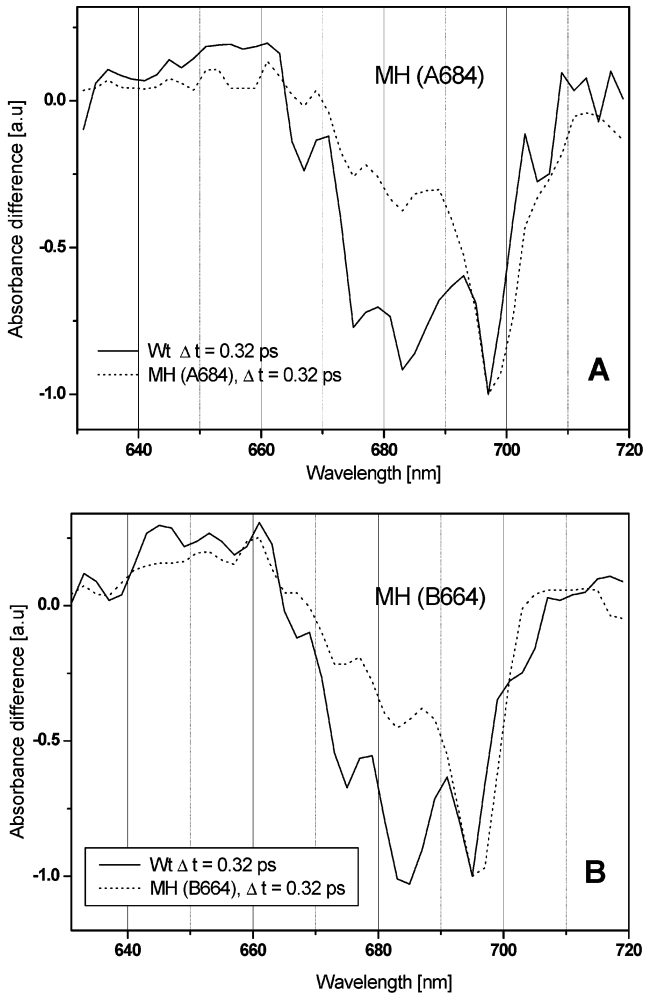

FIGURE 6: Absorbance difference spectra of WT and A_0 mutants [MH(A684) (panel A) and MH(B664) (panel B)] at 20 K measured ~0.32 ps after excitation and normalized to the same amplitude at 695 (697) nm. The difference between mutants and WT demonstrates the loss of excitonic coupling between Chls in the respective mutated branches. See text for details.

DISCUSSION

In this work we have investigated the effect of mutation of the axial ligand to the Chls, eC-A3/eC-B3, attributed to

A_0 of the A-branch and the B-branch, respectively, on electron transfer. The results indicate that mutations cause a block, or significant slow, in electron transfer between A_0 and A_1 and that approximately 40−60% of A_0^- can be photoaccumulated under neutral conditions. These results indicate that in *Chlamydomonas* both the A-branch and the B-branch of the ETC are active, at least through to A_0.

Replacement of the axial ligand to eC-A3 or eC-B3 in *Chlamydomonas* results in a significant alteration in growth phenotype and PSI accumulation (Figure 1). Substitution of the Met with basic (His), polar (Ser), and nonpolar (Leu) amino acids results in poor autotrophic growth even under low (moderate) light intensities in the presence of oxygen. The mutants MH(B664) and ML(B664) fail to grow both autotrophically and heterotrophically under high light in the presence of oxygen, whereas the equivalent mutants of the eC-A3 Chl grow slowly under heterotrophic conditions and only very slowly under autotrophic conditions. However, all the mutants grow anaerobically, suggesting that growth inhibition under aerobic conditions is due to increased sensitivity to photooxidative damage. This demonstrates that a functional PSI complex is present in each mutant but that the site-directed changes introduced into the PSI core result in increased oxygen sensitivity. The results also indicate that the B-side mutants are more susceptible to damage than the corresponding A-side mutants. Recent results from Fairclough et al. (*23*) also indicate that the PsaB-side mutations affect growth more severely. However, they also show that the MH(B664) mutant cannot grow even anaerobically. This is an important difference in results that needs to be resolved.

It is possible that the production of reactive oxygen species under high light in aerobic conditions is responsible for the photooxidative damage of PSI. Fisher et al. (*24*) and Purton et al. (*25*) reported this similar phenomenon for site-directed changes in PsaC and PsaA and suggest that this may result from PSI-mediated reduction of oxygen to form free radical species. A decrease in the level of PSI is not the cause of increased photooxidative damage in this case because the MH(B664) and MS(B664) mutants accumulate PSI to the same level as wild type. Interestingly, replacement of Met by the structurally similar Leu drastically decreased the extent of stable accumulation of PSI complexes in the thylakoid membrane (Figure 2). This might indicate that the coordination of the central Mg of Chls eC-A3 and eC-B3 is important, even if such coordination is weak as in the case of the sulfur ligand provided by Met.

Whether one or two phylloquinones are active in PSI is an area of considerable debate. EPR studies have consistently shown photoaccumulation of a single quinone, supporting arguments that only one branch of the ETC is active (*8*). Calculations based on results from spin-polarized EPR studies of single crystals indicated that the distance between the $P_{700}^+A_1^-$ radical pairs was most consistent with a reduced A-side phylloquinone. In contrast, time-resolved optical measurements of the rate of phylloquinone oxidation in whole cells of green alga showed two rates of oxidation, with $t_{1/e} = 13$ and 140 ns (*11*). Initially, the biphasic kinetics were interpreted as reflecting a low equilibrium constant between A_1 and F_X, leading to a fast redox equilibrium of A_1 and F_X and a slower decay of this quasi-equilibrium state associated with electron transfer from F_X to F_A/F_B (*1*, *11*). However, the kinetic phases were found not to be sensitive to changes in the membrane potential, and alternative models were proposed that include one in which two structurally different equilibrium PSI populations have different kinetics of A_1 reoxidation or one in which there are two active quinones in PSI (suggesting bidirectional electron transfer) (*1*). The latter interpretation is favored on the basis of an analysis of mutants in which the PsaA- or PsaB-side phylloquinone binding pockets (*12*) were used to assign the fast (≈13 ns) component to the reoxidation of the phylloquinone on the PsaB side and the slow (≈140 ns) component to the reoxidation of the phylloquinone on the PsaA side.

To further verify the hypothesis that electron transfer can occur along the A-branch and the B-branch, we have measured absorbance difference spectrum of PSI from MH(A684) and MH(B664) a few hundreds of picoseconds after excitation, when excitation energy is already trapped by the RC. The Δ*A* spectrum at these delay times contains contributions only from charge-separated states. In the WT PSI, charge separation occurs in 20−30 ps (*18*, *26*). Then, P_{700}^+ lives for milliseconds (*27*), and A_0^- transfers an electron to a phylloquinone A_1 in ∼13−21 ps (*28*, *29*). The electron stays on A_1 for nanoseconds (*11*, *12*, *27*) before it is transferred to further electron acceptors. If electron transfer from A_0 to A_1 is blocked, charge recombination between P_{700}^+ and A_0^- occurs in 20−50 ns (*27*). The $(A_1^- - A_1)$ Δ*A* spectrum does not contribute to the Δ*A* signal in the spectral region studied in this work. Therefore, the only states detected by transient absorption spectroscopy on the hundreds of picoseconds time scale are $P700^+$ or $P_{700}^+A_0^-$ (if electron transfer to A_1 is blocked). Figure 3 demonstrates a significant difference between the Δ*A* spectrum for the wild type, the MH(A684) mutant, and the MH(B664) mutant. The shape of the Δ*A* signal for the wild type agrees well with the shape of $(P_{700}^+ - P_{700})$ from the literature (*18*, *21*, *22*). The signals for MH(A684) and MH(B664) are significantly different. It seems unlikely that mutation of the A_0 ligand changes the $(P_{700}^+ - P_{700})$ Δ*A* spectrum so dramatically [the $(P_{700}^+ - P_{700})$; in fact, the Δ*A* spectrum measured on the millisecond time scale for the mutants at room temperature is similar to that of WT (not shown)]. Even mutations of the P_{700} ligands do not introduce such significant spectral changes (*4*, *5*). So, we have assumed that the $(P_{700}^+ - P_{700})$ Δ*A* spectrum was the same for the mutant as for the WT and subtracted the latter from the Δ*A* spectrum measured for the mutants. As a control experiment we have measured the $(A_0^- - A_0)$ Δ*A* spectrum for each mutant (PsaA and PsaB) under reducing conditions (Figure 4). Comparison of the shapes of the ΔΔ*A* spectra obtained by subtraction performed for WT and mutant traces in Figure 4 demonstrates that they are the same within experimental error (Figure 4). The straightforward implication of this is that ΔΔ*A* in Figure 4 comes from $(A_0^- - A_0)$. As the mutation is in either branch A or branch B and the amplitude of the ΔΔ*A* trace in Figure 5 is about twice that in Figure 3, it is very reasonable to propose that the ΔΔ*A* trace in Figure 3 comes from $(A_0^- - A_0)$ in either the A- or B-branch due to an electron transfer block between A_0^- and A_1.

The results strongly support a model for PSI in which electron transfer can occur down either the PsaA or the PsaB branch; comparison of the ΔΔ*A* signals of the A- and the B-side A_0 mutants indicates a branching ratio of approximately 1:1 (Figure 3). This is slightly different from

the ratio of ~2:1 proposed by Guergova-Kuras et al. (*12*), based upon analysis of the amplitudes of the fast and slow phases of A_1 reoxidation, but probably not significantly different when considering that subtraction of spectra is required to observe A_0^-. Finally, it should be underlined that the shape of the $\Delta\Delta A$ spectrum assigned ($A_0^- - A_0$) in the MH(A684) and MH(B664) agrees well with those measured for WT PSI from *C. reinhardtii* (*21*, *22*), but its maximum is 2−5 nm blue shifted compared to the ($A_0^- - A_0$) ΔA maximum for the cyanobacterium *Synechocystis* sp. PCC 6803 (*22*, *28*, *29*). This spectroscopic difference between *C. reinhardtii* and *Synechocystis* may suggest some structural difference in RCs of these two PSIs.

In the WT PSI, the initial ΔA bands peaking at ~675 and ~685 nm measured 300 fs after excitation are associated with excitonic interaction between the eC-A2 and A_0 Chls and between the A_0 Chls and connecting Chls, respectively, in both branches (*30*). However, the 695 nm band observed when exciting at 700 nm is contributed largely by a species that is independent of the excitonically coupled system of Chls, as concluded from the fact that excitation at 705 or 710 nm results in a dramatic decrease of the amplitude of this band. In the cases of both A_0 mutants, the amplitudes of the 675 and 683 nm bands drop about twice relative to the 695 nm bands and compared to the WT PSI (Figure 6). The decrease in amplitude of the 675 and 683 nm bands in PsaA and PsaB mutants is interpreted in terms of disturbance of normal excitonic interactions in respective branches of A_0 PSI mutants. In particular, interactions between A_0 and its closest neighbors, the accessory Chl and connecting Chl, responsible in our model for 675 and 683 nm bands (*30*), are expected to be affected by the mutations in a similar ways: change of position/orientation of the A_0 Chl in either the A- or B-branch reduces its interaction energies with neighbors, and thus, the components of either the A- or B-branch are no longer excitonically coupled. In consequence, the observed ΔA signals at 675 and 683 nm are proposed to come from branch B only for the MH(A684) mutant and from branch A only for MH(B664). This explains the ~2-fold drop of the amplitudes. Thus, the block or slow in electron transfer between A_0 and A_1 may at least be in part due to a change in orientation.

CONCLUSIONS

In the present investigation we have shown that the mutation of the axial ligand to the PsaA-branch (MetA684) and PsaB-branch (MetB664) A_0 Chls disturbs electron transfer between A_0 and A_1. Ultrafast transient absorbance measurements show that A_0^- accumulates in mutant PSI under neutral conditions, demonstrating that electron transfer between A_0^- and A_1 is blocked or significantly slowed. The initial time-resolved spectra also indicate that there is also loss of excitonic coupling between the A_0 Chl and its closest neighbor, the accessory Chl and connecting Chl in both branches. These results strongly indicate that both the A-branch and the B-branch of the ETC are active and support the view of bidirectional electron transfer in *Chlamydomonas* PSI.

REFERENCES

1. Brettel, K., and Liebl, W. (2001) *Biochim. Biophys. Acta 1507*, 100−114.
2. Fromme, P., Jordan, P., and Krauss, N. (2001) *Biochim. Biophys. Acta 1507*, 5−31.
3. Jordan, P., Fromme, P., Klukas, O., Witt, H. T., Saenger, W., and Krauss, N. (2001) *Nature 411*, 909−917.
4. Webber, A. N., Su, H., Bingham, S. E., Käss, H., Krabben, L., Kuhn, M., Schlodder, E., and Lubitz, W. (1996) *Biochemistry 35*, 12857−12863.
5. Krabben, L., Schlodder, E., Jordan, R., Carbonera, D., Giacometti, G., Lee, H., Webber, A. N., and Lubitz, W. (2000) *Biochemistry 39*, 13012−13025.
6. Zech, S. G., Hofbauer, W., Kamlowski, A., Fromme, P., Stehlik, D., Lubitz, W., and Bittl, R. (2000) *J. Phys. Chem. B 104*, 9728−9739.
7. Bittl, R., and Zech, S. G. (2001) *Biochim. Biophys. Acta 1507*, 194−211.
8. Yang, H., Shen, G., Schluchter, W. M., Zybailov, B. L., Ganago, A. O., Vassiliev, I. R., Bryant, D. A., and Golbeck, J. H. (1998) *J. Phys. Chem. B 102*, 8288−8299.
9. Muhiuddin, I. P., Heathcote, P., Carter, S., Purton, S., Rigby, S. E., and Evans, M. C. (2001) *FEBS Lett. 503*, 56−60.
10. Rigby, S. E., Muhiuddin, I. P., Evans, M. C., Purton, S., and Heathcote, P. (2002) *Biochim. Biophys. Acta 1556*, 13−20.
11. Joliot, P., and Joliot, A. (1999) *Biochemistry 38*, 11130−11136.
12. Guergova-Kuras, M., Boudreaux, B., Joliot, A., Joliot, P., and Redding, K. (2001) *Proc. Natl. Acad. Sci. U.S.A. 98*, 4437.
13. Lee, H., Bingham, S. E., and Webber, A. N. (1998) in *Methods in Enzymology*, Vol. 297, pp 311−319, Academic Press, Boca Raton, FL.
14. Boynton, J. E., Gillham, N. W., Harris, E. H., Hosler, J. P., Johnson, A. M., Jones, A. R., Randolph-Anderson, B. L., Robertson, D., Klein, T. M., Shark, K. B., and Sanford, J. C. (1988) *Science 240*, 1534−1538.
15. Webber, A. N., Gibbs, P. B., Ward, J. B., and Bingham, S. E. (1993) *J. Biol. Chem. 268*, 12990−12995.
16. Chua, N. H., and Bennoun, P. (1975) *Proc. Natl. Acad. Sci. U.S.A. 72*, 2175−2179.
17. Cui, L., Bingham, S. E., Kuhn, M., Käss, H., Lubitz, W., and Webber, A. N. (1995) *Biochemistry 34*, 1549−1558.
18. Gibasiewicz, K., Ramesh, V. M., Melkozernov, A. N., Lin, S., Woodbury, N. W., Blankenship, R. E., and Webber, A. N. (2001) *J. Phys. Chem. B 105*, 11498−11506.
19. Gibasiewicz, K., Ramesh, V. M., Lin, S., Woodbury, N. W., and Webber, A. N. (2002) *J. Phys. Chem. B 106*, 6322−6330.
20. Freiberg, A., Timpmann, K., Lin, S., and Woodbury, N. W. (1998) *J. Phys. Chem. 102*, 10974−10982.
21. Melkozernov, A. N., Su, H., Lin, S., Bingham, S., Webber, A. N., and Blankenship, R. E. (1997) *Biochemistry 36*, 2898−2907.
22. Hastings, G., Hoshina, S., Webber, A. N., and Blankenship, R. E. (1995) *Biochemistry 34*, 15512−15522.
23. Fairclough, W. V., Forsyth, A., Evans, M. C. W., Rigby, S. E. J., Purton, S., and Heathcote, P. (2003) *Biochim. Biophys. Acta 1606*, 43−55.
24. Fisher, N., Setif, P., and Rochaix, J. D. (1997) *Biochemistry 36*, 93−102.
25. Purton, S., Stevens, D. R., Muhiuddin, I. P., Evans, M. C. W., Carter, S., Rigby, S. E. J., and Heathcote, P. (2001) *Biochemistry 40*, 2167−2175.
26. Melkorzernov, A. N., Su, H., Webber, A. N., and Blankenship, R. E. (1998) *Photosynth. Res. 56*, 197−207.
27. Brettel, K. (1997) *Biochim. Biophys. Acta 1318*, 322−373.
28. Hastings, G., Kleinherenbrink, F. A. M., Lin, S., McHugh, T. J., and Blankenship, R. E. (1994) *Biochemistry 33*, 3193−3200.
29. Savikhin, S., Xu, W., Soukoulis, V., Chitnis, P. R., and Struve, W. (1999) *Biophys. J. 76*, 3278−3288.
30. Gibasiewicz, K., Ramesh, V. M., Lin, S., Redding, K., Woodbury, N. W., and Webber, A. N. (2003) *Biophys J. 85*, 2547−2559.

BI0354177